

Development in DIII-D of High Beta Discharges Appropriate for Steady-state Tokamak Operation With Burning Plasmas

J.R. Ferron 1), V. Basiuk 2), T.A. Casper 3), C.D. Challis 4), J.C. DeBoo 1), E.J. Doyle 5), Q. Gao 6), A.M. Garofalo 1), C.M. Greenfield 1), C.T. Holcomb 3), A.W. Hyatt 1), S. Ide 7) T.C. Luce 1), M. Murakami 8), Y. Ou 9), J.-M. Park 8), T.W. Petrie 1), C.C. Petty 1), P.A. Politzer 1), H. Reimerdes 10), E. Schuster 9), M. Schneider 2), and A. Wang 5)

- 1) General Atomics, P.O. Box 85608, San Diego, California 91286-5608, USA
- 2) CEA-Cadarache, Cadarache, France
- 3) Lawrence Livermore National Laboratory, Livermore, California 94550, USA
- 4) UKAEA Fusion Culham Science Centre, United Kingdom
- 5) University of California, Los Angeles, California, USA
- 6) Southwest Institute of Physics, Chengdu, China
- 7) Japan Atomic Energy Agency, Naka, Japan
- 8) Oak Ridge National Laboratory, Oak Ridge, Tennessee 37831, USA
- 9) Lehigh University, Bethlehem, Pennsylvania 18015, USA
- 10) Columbia University, New York, New York, USA

e-mail contact of main author: ferron@fusion.gat.com

Abstract. Ideally, tokamak power plants will operate in steady-state at high fusion gain. Recent work at DIII-D on the development of suitable high beta discharges with 100% of the plasma current generated noninductively ($f_{NI} = 1$) is described. In a discharge with $1.5 < q_{min} < 2$, a scan of the discharge shape squareness was used to find the value that maximizes confinement and achievable β_N . A small bias of the up/down balance of the double-null divertor shape away from the ion $B \times \nabla B$ drift direction optimizes pumping for minimum density. Electron cyclotron current drive with a broad deposition profile was found to be effective at avoidance of a 2/1 NTM allowing long duration at $\beta_N = 3.7$. With these improvements, surface voltage $\approx 0-10$ mV, indicating $f_{NI} \approx 1$, was obtained for $0.7 \tau_R$ (resistive time). Stationary discharges with $\beta_N = 3.4$ and $f_{NI} \approx 0.9$ that project to $Q = 5$ in ITER have been demonstrated for τ_R . For use in development of model based controllers for the q profile, transport code models of the current profile evolution during discharge formation have been validated against the experiment. Tests of available actuators confirm that electron heating during the plasma current ramp up to modify the conductivity is by far the most effective. The empirically designed controller has been improved by use of proportional/integral gain and built-in limits to β_N to avoid instabilities. Two alternate steady-state compatible scenarios predicted to be capable of reaching $\beta_N = 5$ have been tested experimentally, motivated by future machines that require high power density and neutron fluence. In a wall stabilized scenario with $q_{min} > 2$, $\beta_N = 4$ has been achieved for $2 s \approx \tau_R$. In a high internal inductance scenario, which maximizes the ideal no-wall stability limit, $\beta_N \approx 4.8$ has been reached with $f_{NI} > 1$.

1. Introduction

A research focus at DIII-D is the development of methods for reliable production of high beta discharges suitable for power plant operation at high fusion gain with 100% of the plasma current generated noninductively (noninductive fraction $f_{NI}=1$) [1]. Recent work has encompassed a complete discharge scenario, from feedback control of the q profile evolution [2] during the initial, low beta, discharge formation phase to the optimization of the discharge shape and electron cyclotron current drive (ECCD) deposition profile for stable, stationary operation at maximum β_N of the $f_{NI}=1$ phase of the discharge. In addition, experiments to increase β_N to 4–5 with profiles suitable for steady-state operation have begun, motivated by the requirement for high power density and neutron fluence in a demonstration power plant. Two approaches capable of reaching $\beta_N=5$ have been identified through modeling and tested

experimentally: a wall stabilized scenario with $q_{\min} > 2$ [3] and a high internal inductance (l_i) scenario [4–6] that maximizes the ideal no-wall stability limit.

2. High f_{NI} Discharges With $q_{\min} > 1.5$

The steady-state compatible scenario that has been the most intensely studied in DIII-D has $1.5 < q_{\min} < 2.0$, $q(0) - q_{\min} < 0.5$ and $q_{95} \approx 5$ [1]. Previously reported discharges of this type have the ohmic loop voltage ≈ 0 –10 mV, with analysis showing that $\approx 100\%$ of the current is driven noninductively, for up to 0.7 s. Transport code analysis found the bootstrap current fraction $f_{\text{BS}} \approx 0.5$ –0.6, with the remainder of the current resulting from electron cyclotron (ECCD) and neutral beam current drive (NBCD). In these $f_{\text{NI}} \approx 1$ discharges the current profile continues to slowly evolve. In contrast, previously reported [7] discharges with $f_{\text{NI}} \approx 0.9$ have a nearly stationary current profile, as indicated by constant values of the field line pitch angle measurements from the MSE diagnostic, for about 1.5 s or $0.9 \tau_{\text{R}}$ (resistive current relaxation time). The duration of the high-performance phase in these $f_{\text{NI}} = 0.9$ –1.0 discharges was limited by the available ECCD pulse length or the appearance of a 2/1 neoclassical tearing mode (NTM).

The expanded ECCD capability (five 110 GHz gyrotrons injecting a total of ≈ 3 MW for 5 s) that became available for 2007–2008 enabled improved operation in this discharge scenario. The higher power, longer pulse ECCD enabled extension of the phase with a stationary current profile in discharges with $f_{\text{NI}} \approx 0.9$ to 2.5 s which is $\approx \tau_{\text{R}}$ at the higher electron temperature resulting from the higher ECCD power (Figs 1,2). The performance factor G [Fig. 1(c)] [8] is equal to the value required for $Q=5$ in ITER with $\beta_{\text{N}} = 3.4$, $H_{89} = 2.3$ and $H_{98y2} = 1.4$. The limit to the duration of the stationary phase is now the total energy available from the neutral beams.

An increase in the stable, stationary value of β_{N} accessible in these discharges was also made possible by the increased total number of gyrotrons and the available ECCD power. By depositing the ECCD with a relatively broad profile, the discharges could be operated reproducibly without the appearance of a 2/1 NTM. A set of discharges demonstrating this effect in a single-null divertor ITER-like plasma shape [9], where the 2/1 NTM occurred at relatively low β_{N} , is shown in Fig. 3. In the discharge shown in red, there is no ECCD and the $n=1$ mode appears soon after β_{N} reaches 3. In the discharge with ECCD (blue), there is no

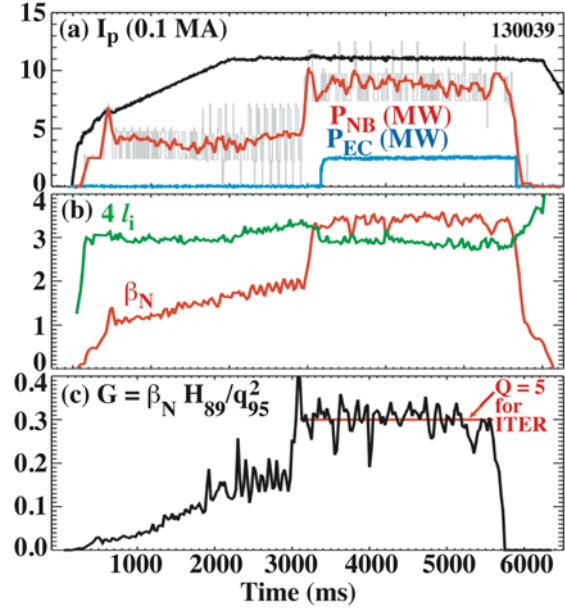


FIG. 1. Time evolution of parameters in a discharge with a stationary current density profile for τ_{R} and $f_{\text{NI}} = 0.9$.

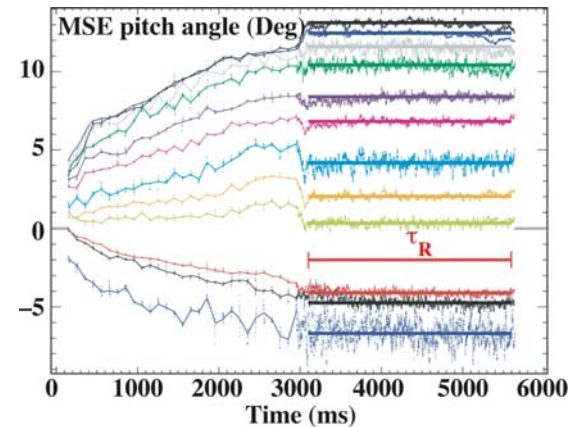


FIG. 2. For the discharge shown in Fig. 1, field line pitch angles at 12 different positions across the radial profile of the plasma measured with the motional Stark effect diagnostic.

$n=1$ mode apart from a brief burst, while in the discharge in which the ECCD is turned off early (black), the $n=1$ mode appears before the end of the high β_N phase.

A broad ECCD deposition profile, as shown in Fig. 4, was found to be essential to maintaining $n=1$ NTM stability. In a separate set of discharges, deposition peaked at $\rho=0.4$ or 0.5 was compared with ECCD distributed between $\rho=0.35$ and 0.55 . In all three cases, $\beta_N=3.2$ was stable for τ_R , but only the case with the broad deposition profile was stable at higher beta, $\beta_N=3.4$. It is not necessary for the broadly deposited ECCD to align with the $q=2$ surface in order to improve the $2/1$ mode stability, as has been the case in previous studies of NTM stabilization with ECCD [10], indicating that current profile tailoring plays a role.

In order to increase the duration and reproducibility of the $f_{NI}=1$ phase in these discharges, a study was made of the effect of the discharge shape on the discharge performance. The resulting optimized discharge shape maximizes the energy confinement and makes a compromise between maximizing the β_N stable to ideal low n modes and minimizing the electron density (for the most ECCD current). To operate at the highest possible β_N , an up/down balanced double-null divertor shape has been shown to be optimum [11]. However, the minimum density is obtained with the DIII-D divertor cryopump geometry by adding a slight bias of the double null shape in the direction opposite to the ion $B \times \nabla B$ drift direction (Fig. 5). The magnitude of the necessary bias, $dR_{sep}=0.5$ cm, is relatively small. This change in the discharge shape was found to have no measurable effect on the energy confinement.

Small changes in the discharge shape squareness were found to have a significant effect on the achievable β_N [12] and the energy confinement. The study focused on the squareness because the elongation and triangularity are largely determined by matching the shape to the divertor

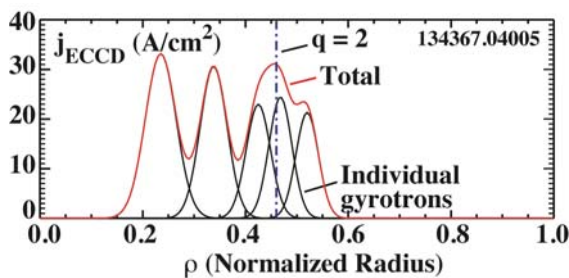


FIG. 4. The calculated ECCD current density radial profile for the discharge shown in blue in Fig. 3.

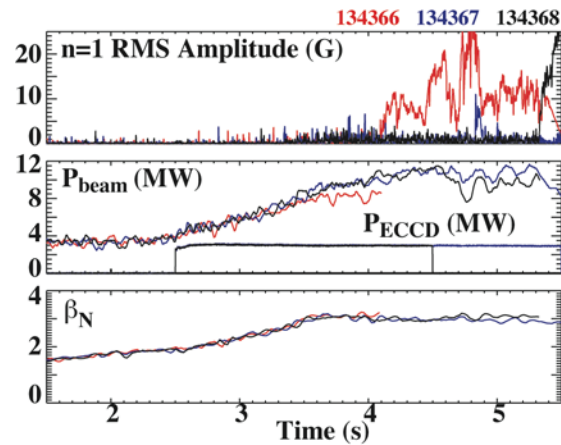


FIG. 3. Time evolution of parameters in three discharges that demonstrates the stabilizing effect of the broadly deposited ECCD on the $2/1$ NTM. Red curves: discharge without ECCD. Blue curves: discharge with ECCD through the entire pulse. Black curves: discharge in which the ECCD turns off at 4.5 s.

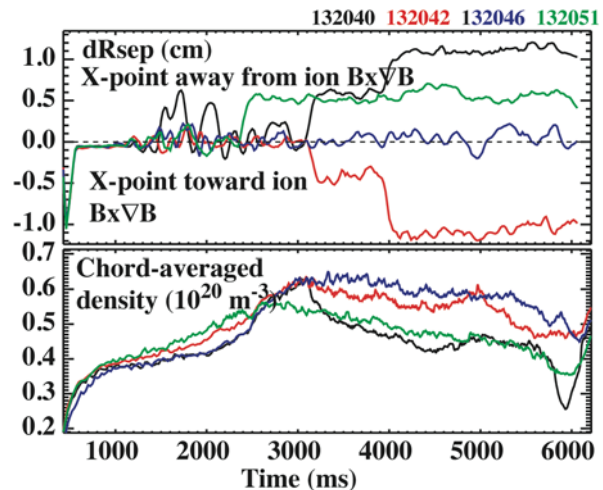


FIG. 5. Four discharges with different values of dR_{sep} beginning at 3 s and the resulting line average density. dR_{sep} is the distance at the outer midplane between the flux surfaces passing through the two X points in the near double null divertor shape.

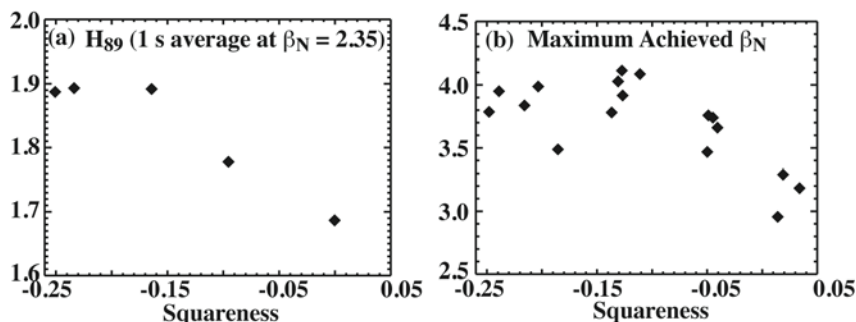


FIG. 6. Results from a scan of discharge squareness using the plasma shapes shown in Fig. 7. (a) Normalized confinement H_{89} averaged over 1 s in discharges with β_N regulated at 2.35, (b) maximum achieved β_N .

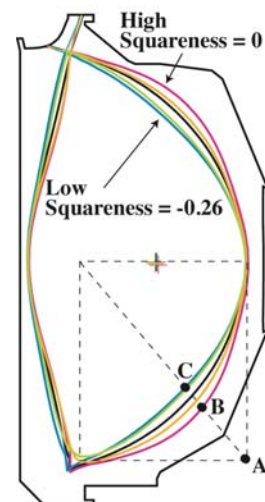


FIG. 7. The discharge shapes used to obtain the results in Fig. 6. Squareness is BC/AB where point B is on an ellipse with the same triangularity and elongation as the discharges shown.

geometry. The results are summarized in Fig. 6 for the five different shapes shown in Fig. 7. Both the maximum achieved β_N and the normalized confinement are optimized at a value of squareness near -0.15 , with β_N and confinement decreasing at higher values and little change observed at lower values.

By utilizing the available neutral beam power, and the ECCD to maintain 2/1 NTM stability, discharges were reproducibly operated at $\beta_N=3.7$. This is in contrast to previously reported high f_{NI} discharges, which had β_N up to 3.4 and were commonly limited in duration by an $n=1$ NTM. Discharges with $V_{loop} \approx 0-10$ mV for increased duration were produced by reducing the plasma current from the typical value of 1.1 MA to 0.9 MA in order to approximately match the total noninductive current (Fig. 8). The higher current discharge is typical of those that have $f_{NI}=0.9$. In the lower current discharge, the duration of the low V_{loop} phase is $0.7 \tau_R$, increased from $0.4 \tau_R$ in the best previously reported case [1]. The reduced current, though, results in the reduced value of the performance factor G . The present limit to the noninductively driven current is the available neutral beam and ECCD power and the limit to duration is the available neutral beam energy.

3. $\beta_N > 4$ in Discharges With Increased l_i

An alternative steady-state compatible scenario is based on a discharge with a relatively high value of l_i (1.1–1.5) indicating a peaked current profile [4–6]. In this range of l_i , plasmas with $\beta_N=4-5$ are expected to be stable to low n ideal kink modes even without the stabilizing effect of a conducting vacuum vessel. Thus a reactor based on this type of high β_N discharge would not require rotation or additional hardware for feedback stabilization of resistive wall modes. There are challenges to maintaining an elevated value of l_i in steady-state because of

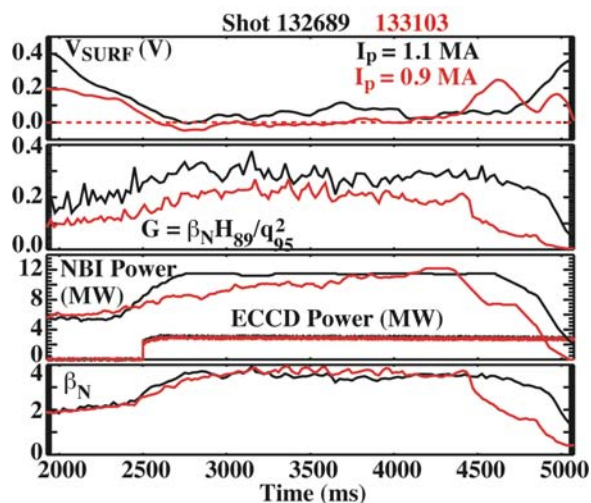


FIG. 8. Surface voltage, fusion gain factor, neutral beam and ECCD powers and β_N evolution in two discharges with different plasma current. The lowest current discharge has surface voltage consistent with $f_{NI} \approx 1.0$.

the broad bootstrap current profile that would be produced in a high β_N H-mode discharge. A self-consistent scenario with relatively modest parameters, $l_i \approx 1$ and $\beta_N = 3.5\text{--}4.0$, was proposed in [6]. In the experimental work discussed here, the goal is to investigate the MHD stability of equilibria with β_N near 5, $l_i > 1$, and parameters compatible with high bootstrap current fraction operation. The current profile in these high β_N discharges is not yet stationary; this is the next step in the development of this scenario.

An initial, low β_N equilibrium was established by starting the discharge in ohmic or L-mode conditions at low T_e and remaining in these conditions long enough for the current profile to evolve to a stationary state (Fig. 9). Because T_e , and thus the conductivity, was very low in the outer half of the plasma, and almost all current was driven inductively, l_i reached a relatively large asymptotic value. The onset of sawtooth oscillations limited $q(0)$ to 1, so that $J(0)$, and thus the asymptotic value of l_i , was a function of I_p/B_T . During the experiment, a scan in I_p/B_T was performed, resulting in target values of l_i that varied from 1.65 to 1.35 [Fig. 9(b)] as I_p/B_T was changed from 0.4 to 0.65 [Fig. 9(a)]. ECCD deposited at $\rho \approx 0.3$ was added starting at 1.7 s in order to make a small (≈ 0.1) predicted increase in l_i and to increase T_e to reduce the rate at which the current profile would change after the start of the high β_N phase. Initially, $dR_{\text{sep}} = 2.5$ cm in the near-double-null plasma shape in order to hold the discharge in L-mode in the neutral beam injection phase beginning at 2.5 s. At 2.8 s, dR_{sep} is changed to zero to trigger the H-mode transition and produce an up/down balanced double-null plasma shape which is expected have the highest β_N limit. This results in a transient increase in l_i . As β_N and the bootstrap current fraction increase, and the neutral beam power saturates at the maximum available value [Fig. 9(c)], l_i decreases until it reaches an equilibrium value toward the end of the high-performance phase.

The best high β_N performance (Fig. 10) was observed at a midrange value of I_p/B_T (0.8 MA/1.7 T). In the discharge shown in the figure, $\beta_N \approx 4.8$ was maintained for about 0.4 s, while l_i drops from 1.25 to 1.0, and β_N remains above 4 for 1 s. Confinement is well above the standard H-mode value, as was

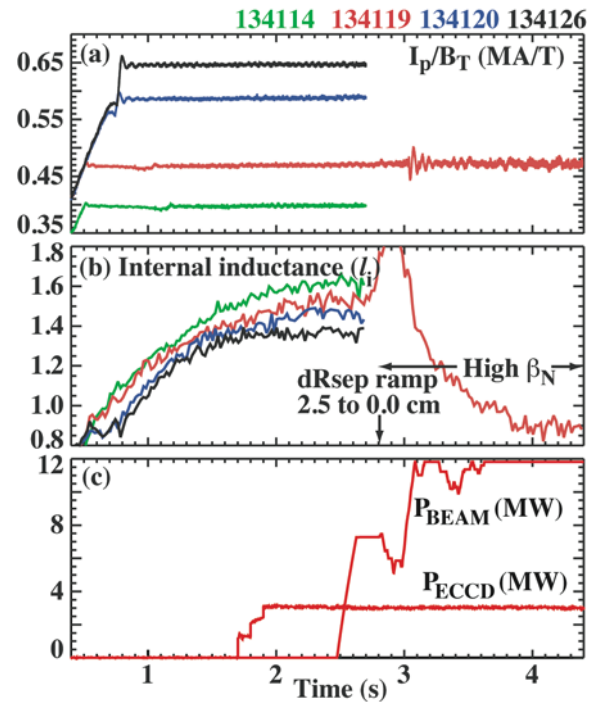


FIG. 9. Formation of the discharges with a high value of l_i . The red curve shows parameters for the discharge shown on an expanded scale in Fig. 10.

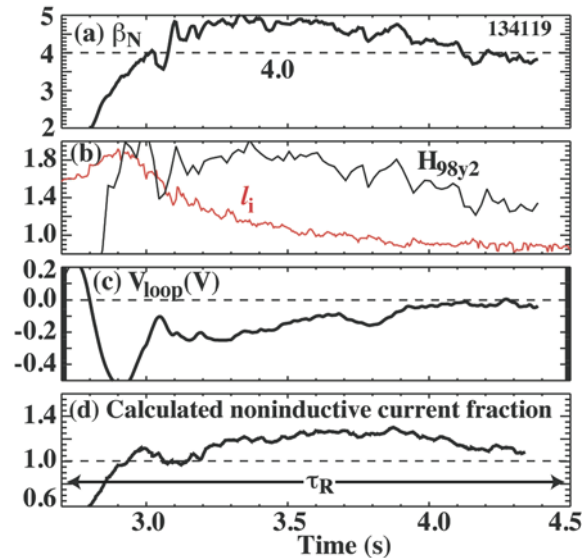


FIG. 10. Time evolution of the high-performance phase in a discharge with $I_p/B_T = 0.8$ MA/1.7 T and a high initial value of l_i . The noninductive current fraction was calculated using the ONETWO transport code.

observed in previous high l_i experiments [4,5], with H_{98y2} up to 1.8 [Fig. 10(b)] and $H_{89}\approx 2.6$. The performance factor $G\approx 0.23$, the same as in the lowest current discharge shown in Fig. 8, although the current for the discharge in Fig. 10 is even lower. The total noninductively driven current is larger than I_p , as indicated by surface voltage [Fig. 10(c)] which remains negative throughout the high β_N phase. The calculated value of f_{NI} is as high as 1.2, with 90% resulting from bootstrap current during the highest β_N phase.

The MHD activity is dominantly $n=1$, beginning with fishbone-type instabilities changing to bursts of $n=1$ activity of varying length, some with especially large amplitude growing in less than 1 ms. Large amplitude, fast-growing bursts of this type resulted in brief collapses during the initial β_N rise, Fig. 10(a). The high performance phase is terminated by the onset of a 2/1 NTM at 4.4 s. A discharge at higher I_p/B_T (1.1 MA/1.7 T) at the time of the peak $\beta_N=4.6$ ($l_i=1.2$) was calculated to be stable to the ideal $n=1$ kink without a conducting wall. The pressure gradient was calculated to be only slightly below the value marginally stable to the infinite- n ballooning mode across the full radial profile (Fig. 11).

4. High β_N , Wall-stabilized Discharges With $q_{\min}>2$

In contrast to the high l_i scenario described in the previous section, an alternative approach to stable operation with $\beta_N=4-5$ has a very broad current profile, low $l_i\approx 0.6$, and $q_{\min}>2$. As reported previously [3], $\beta_N=4$ was sustained in this scenario for $2\text{ s}\approx\tau_R$. The broad current profile, created with simultaneous I_p and B_T ramps, improves stability by maximizing the effect of wall stabilization. Thus, this scenario requires that resistive wall modes be stabilized either by active feedback or sufficient toroidal rotation. The bootstrap current fraction is above 0.6, with an off-axis peak near the q_{\min} location, $\rho=0.5$, where there is an internal transport barrier. As a result of the on-axis neutral beam driven current, q_{\min} decreases slowly during the high β_N phase, ending below 2. Recent experiments focused on reduction of the on-axis NBCD, with most neutral beam power injected in the direction opposite to the plasma current, in order to maintain q_{\min} above 2 and move the bootstrap current further off axis by increasing the radial location of q_{\min} . With this approach, $\rho_{q_{\min}}$ was observed to increase slowly with time, reaching ≈ 0.6 . However, as a result of the toroidal rotation profile produced by the dominant counter-direction beam injection, mode locking at low rotation limited β_N to approximately the no-wall limit. Future experiments will utilize sufficient neutral-beam-injected torque throughout the discharge to avoid a low rotation phase.

5. Response of the Current Profile Evolution to Feedback Control Actuators

For the steady-state scenario described in Sec. 2, closed loop feedback control of the evolution of q_{\min} during the I_p ramp up and early flattop is being developed for use in setting the value of q_{\min} at the start of the high β_N phase [2]. In addition to tests of empirically designed controllers, open-loop measurements of the q profile evolution have been compared to transport code simulations to validate the models for poloidal flux evolution and neutral beam

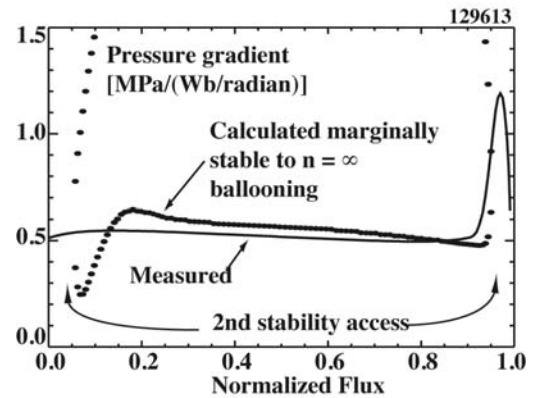


FIG. 11. In a high l_i scenario discharge with $l_i=1.2$ and $\beta_N=4.6$, a comparison between the measured pressure gradient radial profile and the profile calculated to be marginally stable to the infinite- n ballooning mode.

current drive for use in development of model-based real-time controllers [13]. Figure 12 illustrates two different comparisons of the transport code model to the measured q evolution. The left column shows the effect of changing the electron temperature using ECH heating, while the right column shows a measurement of the response of the rate of change of q_{\min} to a step in the neutral beam power. In both cases, the transport code reproduces well the measured q evolution.

Experimental tests of the available actuators have been made in order to compare their effectiveness for modification of the q evolution. By far, the strongest actuator is electron heating to modify T_e , and thus the conductivity and the rate of penetration of the ohmic electric field (left column, Fig. 12). Changes in the I_p ramp rate can be used to alter the ohmic loop voltage and the rate of change of confinement. However, changing the I_p ramp rate has little observed effect on the q_{\min} time evolution. The primary changes in the current density are outside the peak at $\rho \approx 0.4$, so only l_i changes significantly. The electron density can be changed in order to modify T_e for a fixed input power. However, only small variations in n_e are feasible during the I_p ramp up. Changes in the neutral beam voltage or the mixture of co-injection and counter-injection neutral beams were found to be weak actuators for q_{\min} control, primarily because in order to maintain β_N at stable values, limited neutral beam power can be used during the I_p ramp-up so the NBCD fraction is 15% or less.

The q_{\min} evolution was observed to be slightly slower when the beam voltage was reduced from 75 keV to 55 keV. Similarly, the q_{\min} evolution is slightly slower with only co-injection than with balanced co/counter-injection. As discussed in [2], ECCD and fast wave current drive are inefficient during the I_p ramp up as a result of low β and T_e .

Improvements in the empirically designed controller for q_{\min} have been tested. Previously [2], proportional gain control was used to calculate the required neutral beam power (P_{NB}) to vary the rate of evolution of the current profile by changing T_e . This method worked well as long as the q profile measurement was made at sufficiently short intervals (e.g. 10 ms). In order to conserve the available energy of the

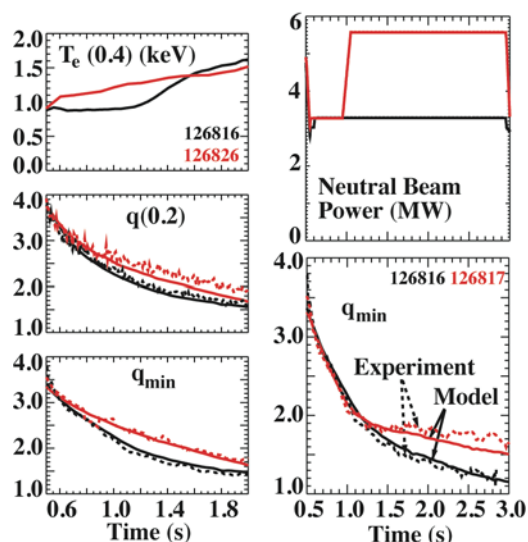


FIG. 12. Comparisons between experiment (dashed) and simulation (solid) using the ONETWO transport code of the q evolution during the I_p ramp up and early flattop. Left column: At two different levels of T_e , varied using ECH heating. Right column: Response of dq_{\min}/dt to a step in P_{NB} .

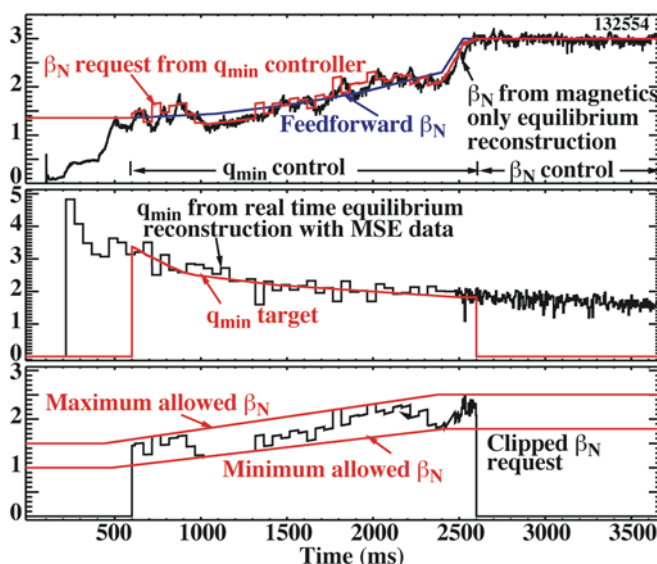


FIG. 13. An example of the improved controller for the time evolution of q_{\min} . Control of q_{\min} is active between 600 ms and 2600 ms. After 2600 ms, β_N is controlled directly to a preprogrammed value.

neutral beam used for the motional Stark effect diagnostic for use during the high β_N phase, during the discharge formation the beam is pulsed with a low duty cycle. The result is infrequent measurements of the q profile and with a measurement interval of 50 ms, a slow oscillation in the controlled value of q_{\min} was observed. The addition of integral gain allowed the proportional gain to be reduced and the integration filters measurement noise. The resulting slow control response is appropriate for the slow q evolution during the I_p ramp up. Testing showed that measurement noise or a slow rate of change of the target q_{\min} could result in a large P_{NB} demand, increasing β_N and triggering a tearing mode. To avoid this, the proportional/integral controller was altered to use the error in q_{\min} to generate a target value for β_N which is then passed to the β_N controller to generate the P_{NB} request (Fig. 13). In this way, the β_N target value can be clipped to remain within a stable window. The controller is further improved by scaling the β_N target value by n_e which effectively results in a request for the average T_e , the intended actuator.

6. Summary

Progress toward reliable operation of high β discharges with $f_{NI}=1$ has been made both by improving the scenario with $1.5 < q_{\min} < 2.0$ and by exploring discharge scenarios that offer the possibility of operation with higher values of β_N . Optimization of the discharge shape for particle pumping, confinement, stability and utilization of the expanded ECCD capability at DIII-D has resulted in $f_{NI} \approx 1$ operation for longer duration, $\approx 0.7\tau_R$, at higher $\beta_N=3.7$. In both the high l_i and broad current profile scenarios, $\beta_N > 4$ for $10 \tau_E$ or longer has been achieved opening the possibility of increased bootstrap current fraction and higher power density reactor operation. Development of the capability for feedback control of the q profile continued with the focus on the q evolution during the discharge formation. The empirically designed controller has been improved to allow avoidance of β_N limits. Comparisons of the measured q evolution with transport code predictions have been used to validate the physics models for development of model-based controllers.

Acknowledgments

This work was supported in part by the US Department of Energy under DE-FC02-04ER54698, DE-AC52-07NA27344, DE-FG02-01ER54615, DE-AC05-00OR22725, DE-FG02-92ER54141, and DE-FG02-89ER53297.

References

- [1] MURAKAMI, M., *et al.*, Plasma Phys. **13**, 056106 (2006).
- [2] FERRON, J.R., *et al.*, Nucl. Fusion **46**, L13 (2006).
- [3] GAROFALO, A.M., *et al.*, Plasma Phys. **13**, 056110 (2006).
- [4] FERRON, J.R., *et al.*, Phys. Fluids B **5**, 2532 (1993).
- [5] LAO, L.L., *et al.*, Plasma Phys. **5**, 1050 (1998).
- [6] LIN-LIU, Y.R., *et al.*, Plasma Phys. **6**, 3934 (1999).
- [7] MURAKAMI, M., *et al.*, Nucl. Fusion **45**, 1419 (2005).
- [8] GORMEZANO, G., *et al.*, Nucl. Fusion **47**, S285 (2007).
- [9] DOYLE, E.J., *et al.*, this conference.
- [11] PRATER, R., *et al.*, Nucl. Fusion **47**, 371 (2007).
- [12] FERRON, J.R., *et al.*, Plasma Phys. **12**, 056126 (2005).
- [13] WADE, M.R., Nucl. Fusion **47**, S543 (2007).
- [14] OU, Y., Fusion Eng. Design **82**, 1153 (2007).